Journal of Sound and Vibration (2002) **252**(4), 697–715
doi:10.1006/jsvi.2001.3674, available online at http://www.idealibrary.com on IDEAL®

RANDOM VIBRATION OF A ROTATING BLADE WITH EXTERNAL AND INTERNAL DAMPING BY THE FINITE ELEMENT METHOD

C.-L. Chen and L.-W. Chen

Department of Mechanical Engineering, National Cheng Kung University, Tainan 70101, *Taiwan, Republic of China. E-mail: chenlw@mail.ncku.edu.tw*

(*Received* 2 *May* 2000, *and in final form* 20 *March* 2001)

The finite element model is employed to investigate the mean-square response of a rotating blade with external and internal damping under stationary or non-stationary random excitation. The blade is considered to be subjected to white-noise and earthquake excitations. The effects of rotational speed, external and internal damping on the mean-square response are studied. It is found that the mean-square response decreases quickly when the external and internal damping increases within some scope. Moreover, the increment of rotational speed will reduce the mean-square response of a rotating blade. It is also found that the mean-square response decreases when the low natural frequency of base decreases. Inversely, the mean-square response increases when the high natural frequency of base (natural frequencies of base are over the first natural frequency of blade) decreases. The reliability of a rotating blade subjected to stationary or non-stationary excitations is also obtained.

1. INTRODUCTION

The random vibration problems of a rotating blade are important in modern turbomachinery design. The blades of turbomachinery are frequently based on random excitations of fluid pressure excitations, earthquake loads, bearing oil excitations, or impact loads. The random response of deterministic or undeterministic system is produced under the random excitation. The over-random response is one of the serious problems which may result in instability or fatigue of the system and should be considered in engineering design. The variable of damping capacity is an important factor to prevent the large consecutive damage due to the over-random response of a blade.

Carnegie [1] studied the vibration of a rotating cantilever blade by using the energy method. The increment of strain energy due to rotation was first investigated. Further studies of the vibrational characteristics of thin rotating blades using the finite difference method are presented by Carnegie *et al.* [2]. Moreover, Carnegie and Rao [3] studied the vibration problems of a rotating blade by the extended Holzer's method. Krupka and Baumanis [4] studied the bending–bending mode of a rotating blade including rotary inertia and shear deflection by the Myklestad method. Stafford and Giurgiutiu [5] used a semianalytic method based on transfer matrix method to study a rotating Timoshenko beam. Abbas [6] and Thomas and Abbas [7] developed a finite element model which can satisfy all the geometric and natural boundary conditions of a thick non-rotating blade. Chen and Chen [8, 9] further studied the vibration and stability of cracked rotating blades

0022-460X/02/$35.00

by the finite element model which can satisfy all the geometric and natural boundary conditions. Zorzi and Nelson [10] studied the effects of external and internal damping on rotor-bearing systems by the finite element model. Fang and Wang [11, 12] studied the mean-square response to white noise excitation of multi-degree-of-freedom (m.d.o.f.) systems by modal analysis. Ahmadi and Satter [13] analyzed the mean-square response of Euler beam under non-stationary random excitation. Lee and Singh [14] developed a new analytical method in order to study the impulse response of discrete vibratory systems. Elishakoff *et al.* [15] studied the random vibrations of beams with various boundary conditions by dynamic-edge-effect method. Fang [16] used the transfer matrix method to study the dynamic behavior of a beam system with uncertain parameters. Lin *et al.* [17] worked on the evolutionary Kanai–Tajimi earthquake models for engineering design purposes. The stochastic response of asymmetric base isolated buildings with the Kanai–Tajimi earthquake excitation were studied by Jangid and Datta [18]. Elishakoff and Zhu [19] developed an improved finite element formulation of beams subjected to random loading. Rackwitz and Fiessler [20] studied the structural reliability under combined random load sequences. The first passage probability for stationary and non-stationary random processes had been discussed by Langley [21] and Mason and Iwan [22]. Cederbaum *et al.* [23] analyzed the random vibration and reliability of plates and shells for the first passage problem.

This report presents the finite element model to solve the response and reliability problems of a rotating blade with external and internal damping under stationary and non-stationary random excitations of white noise and earthquake.

2. FINITE ELEMENT FORMULATION

A rotating cantilever blade of length L subjected to the stationary random excitations of concentrated force $p(t)\delta(x-L)$, distributed force $\bar{p}(x,t)$ and earthquake acceleration $\ddot{y}_0(t)$ (Figure 1) is considered. The Euler thin beam elements which neglect the effect of transverse shear and rotatory inertia are used. The strain energy U and the kinetic energy T of the ith beam element are given by [9–11]

$$U = \int_0^1 \frac{EI}{2l}\left(\frac{\partial^2\psi}{\partial\eta^2}\right)^2 \mathrm{d}\eta, \qquad T = \int_0^1 \frac{1}{2}\rho A l^3 \left(\frac{\partial\psi}{\partial t}\right)^2 \mathrm{d}\eta. \tag{1, 2}$$

We ignore the longitudinal elastic motion of the blade; the work W_4 of the ith beam element due to the centrifugal force is expressed as

$$\begin{aligned} W_4 = &-\int_0^l \left\{\rho A\Omega^2[R_d + (i-1)l + x_i]\frac{1}{2}\left[\int_0^l \left(\frac{\partial y}{\partial x_1}\right)^2 \mathrm{d}x_1 \right.\right. \\ &\left.\left. + \int_0^l \left(\frac{\partial y}{\partial x_2}\right)^2 \mathrm{d}x_2 + \cdots + \int_0^l \left(\frac{\partial y}{\partial x_k}\right)^2 \mathrm{d}x_k + \cdots + \int_0^{x_i} \left(\frac{\partial y}{\partial x_i}\right)^2 \mathrm{d}x_i\right]\right\} \mathrm{d}x_i \\ = &-\frac{EI}{2l}\left\{S_1 \int_0^1 \eta \int_0^\eta \left(\frac{\partial\psi}{\partial\eta}\right)^2 \mathrm{d}\eta\,\mathrm{d}\eta + S_3 \int_0^1 \int_0^\eta \left(\frac{\partial\psi}{\partial\eta}\right)^2 \mathrm{d}\eta\,\mathrm{d}\eta + S_4 \int_0^1 \left(\frac{\partial\psi}{\partial\eta}\right)^2 \mathrm{d}\eta\right\}. \end{aligned} \tag{3}$$

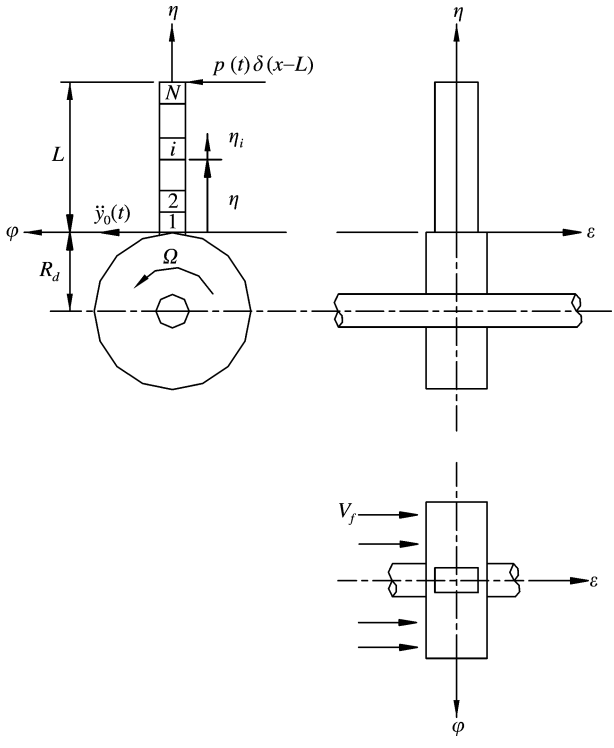

Figure 1. Blade disc assembly.

The virtual work δW on the element due to the conservative and non-conservative forces is expressed as

$$\delta W = \delta W_1 + \delta W_2 + \delta W_3 + \delta W_4, \tag{4}$$

$$\delta W_1 = \int_0^1 l\,[p(t)\delta(\eta - 1) + \bar{p}(\eta, t) - \rho A \ddot{y}_0(t)]\,\delta\psi\,\mathrm{d}\eta. \tag{5}$$

$$\delta W_2 = -\int_0^1 EIl^3 C_0 \left(\frac{\partial \psi}{\partial t}\right) \delta\psi\,\mathrm{d}\eta \tag{6}$$

and

$$\delta W_3 = -\int_0^1 \frac{EI}{l} C_1 \left(\frac{\partial^3 \psi}{\partial t \partial \eta^2}\right) \delta\left(\frac{\partial^2 \psi}{\partial \eta^2}\right) \mathrm{d}\eta, \tag{7}$$

where δW_1 is the virtual work of the random excitations, δW_2 is the virtual work of the external damping force, δW_3 is the virtual work of the internal damping force, l is the element length, ψ is the non-dimensional deflection y/l of the beam neutral line, η is the non-dimensional co-ordinate x/l, R_d is the radius of disc, Ω is the rotational speed of disc, $\delta(\eta - 1)$ is Dirac's delta function, E is the modulus of elasticity, I is the second moment of area of cross-section, ρ is the mass density of the material of blade, A is the cross-sectional area of blade, C_0 is the simplified external damping coefficient, C_1 is the simplified internal

damping coefficient, e is the ratio of disc radius to length of blade R_d/L, and N is the selected element number. The other non-dimensional parameters are defined as

$$S_1 = \rho A l^4 \Omega^2 / EI = \mu / N^4, \quad \text{rotational speed parameter,}$$

$$S_3 = S_1 [e \times N + (i-1)], \qquad S_4 = \sum_{k=1}^{N-1} S_1 \left(e \times N + k + \frac{1}{2} \right).$$

The cubic Hermitian element is adopted. The deflection ψ of the ith beam element can be denoted as

$$\begin{aligned} \psi &= \mathbf{f}(\eta)\mathbf{Y}(t) \\ &= f_1 \psi_i + f_2 \psi_i' + f_3 \psi_{i+1} + f_4 \psi_{i+1}', \end{aligned} \tag{8}$$

where

$$\mathbf{f}(\eta) = [f_1 \quad f_2 \quad f_3 \quad f_4], \tag{9}$$

$$\mathbf{Y}^{\mathrm{T}}(t) = [\psi_i \quad \psi_i' \quad \psi_{i+1} \quad \psi_{i+1}'], \tag{10}$$

$$f_1 = (1 - 3\eta^2 + 2\eta^3), \qquad f_2 = (\eta - 2\eta^2 + \eta^3), \qquad f_3 = (3\eta^2 - 2\eta^3) \tag{11–13}$$

and

$$f_4 = (-\eta^2 + \eta^3). \tag{14}$$

The f_1, f_2, f_3 and f_4 are shape functions. Consequently, the general form of Hamilton's principle for the system is

$$\int_{t_1}^{t_2} (\delta T - \delta U + \delta W)\, \mathrm{d}t = 0. \tag{15}$$

Substituting equations (1)–(8) into equation (15), we have

$$\begin{aligned} \int_{t_1}^{t_2} \Bigg\{ & \rho A l^3 \int_0^1 (\mathbf{f}\ddot{\mathbf{Y}}) \delta(\mathbf{f}\dot{\mathbf{Y}})\, \mathrm{d}\eta - \frac{EI}{l} \int_0^1 (\mathbf{f}''\mathbf{Y}) \delta(\mathbf{f}''\mathbf{Y})\, \mathrm{d}\eta \\ & + \int_0^1 l[p(t)\delta(\eta - 1) + \bar{p}(\eta, t) - \rho A \ddot{y}_0(t)] \delta(\mathbf{f}\mathbf{Y})\, \mathrm{d}\eta \\ & - EIl^3 C_0 \int_0^1 (\mathbf{f}\dot{\mathbf{Y}}) \delta(\mathbf{f}\mathbf{Y})\, \mathrm{d}\eta - \frac{EI}{l} C_1 \int_0^1 (\mathbf{f}''\dot{\mathbf{Y}}) \delta(\mathbf{f}''\mathbf{Y})\, \mathrm{d}\eta \\ & - \frac{EI}{l} \Bigg[S_1 \int_0^1 \eta \int_0^\eta (\mathbf{f}'\mathbf{Y})\, \delta(\mathbf{f}'\mathbf{Y})\, \mathrm{d}\eta\, \mathrm{d}\eta + S_3 \int_0^1 \int_0^\eta (\mathbf{f}'\mathbf{Y}) \delta(\mathbf{f}'\mathbf{Y})\, \mathrm{d}\eta\, \mathrm{d}\eta \\ & + S_4 \int_0^1 (\mathbf{f}'\mathbf{Y}) \delta(\mathbf{f}'\mathbf{Y})\, \mathrm{d}\eta \Bigg] \Bigg\}\, \mathrm{d}t = 0. \end{aligned} \tag{16}$$

Performing the integrals of equation (16), the finite element dynamic differential equation can be obtained in the matrix form as

$$\mathbf{M}_e\ddot{\mathbf{Y}} + \mathbf{C}_e\dot{\mathbf{Y}} + \mathbf{K}_e\mathbf{Y} = \mathbf{F}_e, \tag{17}$$

where $\mathbf{M}_e$ is the element mass matrix, $\mathbf{C}_e$ is the element damping matrix, $\mathbf{K}_e$ is the element stiffness matrix, and $\mathbf{F}_e$ is the element external force vector. The detailed expressions of the matrices are listed in Appendix A.

The boundary conditions at the clamped root are

$$\psi_1 = 0 \quad \text{and} \quad \psi_1' = 0. \tag{18}$$

Equation (17) of each element and the boundary conditions, equation (18), can be assembled to give the finite global equations:

$$\mathbf{M}\ddot{\mathbf{q}} + \mathbf{C}\dot{\mathbf{q}} + \mathbf{K}\mathbf{q} = \mathbf{F}, \tag{19}$$

where $\mathbf{M}$ is the global mass matrix, $\mathbf{C}$ is the global damping matrix, $\mathbf{K}$ is the global stiffness matrix, $\mathbf{F}$ is the global external force vector, and $\mathbf{q}$ is the global co-ordinate vector.

Express equation (19) in state-space form as

$$\begin{bmatrix} \mathbf{C} & \mathbf{M} \\ \mathbf{M} & \mathbf{0} \end{bmatrix} \begin{Bmatrix} \dot{\mathbf{q}} \\ \ddot{\mathbf{q}} \end{Bmatrix} + \begin{bmatrix} \mathbf{K} & \mathbf{0} \\ \mathbf{0} & -\mathbf{M} \end{bmatrix} \begin{Bmatrix} \mathbf{q} \\ \dot{\mathbf{q}} \end{Bmatrix} = \begin{Bmatrix} \mathbf{F} \\ \mathbf{0} \end{Bmatrix} \tag{20}$$

or

$$\mathbf{B}\dot{\boldsymbol{\varepsilon}} + \mathbf{A}\boldsymbol{\varepsilon} = \mathbf{Q}, \tag{21}$$

where

$$\mathbf{B} = \begin{bmatrix} \mathbf{C} & \mathbf{M} \\ \mathbf{M} & \mathbf{0} \end{bmatrix}, \quad \mathbf{A} = \begin{bmatrix} \mathbf{K} & \mathbf{0} \\ \mathbf{0} & -\mathbf{M} \end{bmatrix},$$

$$\boldsymbol{\varepsilon} = \begin{Bmatrix} \mathbf{q} \\ \dot{\mathbf{q}} \end{Bmatrix} \quad \text{and} \quad \mathbf{Q} = \begin{Bmatrix} \mathbf{F} \\ \mathbf{0} \end{Bmatrix}. \tag{22}$$

Let the time-dependent vector $\boldsymbol{\varepsilon}$ be expressed as

$$\boldsymbol{\varepsilon} = \mathbf{U}\mathbf{Z}, \tag{23}$$

where $\mathbf{U}$ is the modal matrix of the equation $\mathbf{B}\dot{\boldsymbol{\varepsilon}} + \mathbf{A}\boldsymbol{\varepsilon} = \mathbf{0}$ and $\mathbf{Z}$ is the time-dependent co-ordinates.

Substituting equation (23) into equation (21), we have

$$\mathbf{B}\mathbf{U}\dot{\mathbf{Z}} + \mathbf{A}\mathbf{U}\mathbf{Z} = \mathbf{Q}. \tag{24}$$

Premultiply both sides of equation (24) by $\mathbf{U}^{\mathrm{T}}$ to obtain

$$\dot{Z}_i + \lambda_i Z_i = G_i(t), \quad i = 1, 2, \ldots, 4N, \tag{25}$$

where

$$\mathbf{U}^{\mathrm{T}}\mathbf{B}\mathbf{U} = \mathbf{D} = diagonal\begin{bmatrix} \ddots & & \\ & D_i & \\ & & \ddots \end{bmatrix},$$

$$\mathbf{U}^{\mathrm{T}}\mathbf{A}\mathbf{U} = \mathbf{P} = diagonal\begin{bmatrix} \ddots & & \\ & P_i & \\ & & \ddots \end{bmatrix},$$

$$\mathbf{Z}^{\mathrm{T}} = [Z_1 \quad Z_2 \quad \cdots \quad Z_i \quad \cdots], \qquad \lambda_i = P_i/D_i$$

and

$$G_i(t) = \frac{1}{D_i}\sum_{j=1}^{4N} U_{ji}Q_j = \frac{1}{D_i}\sum_{j=1}^{2N} U_{ji}F_j. \tag{26}$$

The solution of equation (25) is usually expressed by Duhamel's integral as [17]

$$Z_i = \int_{-\infty}^{\infty} G_i(t-\tau)\, h_i(\tau)\, \mathrm{d}\tau, \tag{27}$$

where

$$h_i(\tau) = \mathrm{e}^{-\lambda_i\tau} \tag{28}$$

and

$$\begin{aligned} H_i(\omega) &= \int_{-\infty}^{\infty} h_i(\tau)\, \mathrm{e}^{-\mathrm{j}\omega\tau}\, \mathrm{d}\tau \\ &= (\lambda_i + \mathrm{j}\omega)^{-1}. \end{aligned} \tag{29}$$

Substituting equation (27) into equation (23), the response y at r points known as the element nodal points can be shown as

$$y = l\sum_{i=1}^{4N} U_{ri}\int_{-\infty}^{\infty} G_i(t-\tau)h_i(\tau)\, \mathrm{d}\tau. \tag{30}$$

2.1. STATIONARY RANDOM EXCITATION

For the Gaussian stationary random processes, the autocorrelation function of the response y is expressed as

$$\begin{aligned} R_y(r,\tau) &= E[y(x,t)y(x,t+\tau)] \\ &= l^2\sum_{i=1}^{4N}\sum_{k=1}^{4N} U_{ri}U_{rk} \\ &\quad \int_{-\infty}^{\infty}\int_{-\infty}^{\infty} h_i(\tau_1)h_k(\tau_2)\, E[G_i(t-\tau_1)\, G_k(t+\tau-\tau_2)]\, \mathrm{d}\tau_1\, \mathrm{d}\tau_2. \end{aligned} \tag{31}$$

According to the Wiener–Khintchine relationship, the spectral function of y is

$$S_y(r,\omega) = \frac{1}{2\pi}\int_{-\infty}^{\infty} R_y(x,\tau)\,\mathrm{e}^{-\mathrm{j}\omega\tau}\,\mathrm{d}\tau$$

$$= \frac{l^2}{2\pi}\sum_{i=1}^{4N}\sum_{k=1}^{4N} U_{ri}U_{rk}H_i(-\omega)\,H_k(\omega)$$

$$\int_{-\infty}^{\infty} E[G_i(t-\tau_1)\,G_k(t+\tau-\tau_2)]\,\mathrm{e}^{-\mathrm{j}\omega(\tau+\tau_1-\tau_2)}\,\mathrm{d}\tau. \tag{32}$$

When the mean values are zero, the mean-square response is expressed as

$$E[y^2] = \int_{-\infty}^{\infty} S_y(r,\omega)\,\mathrm{d}\omega \tag{33}$$

and equation (33) may then be solved when the random excitations are given.

For the white-noise excitation, the spectral function of $p(t)$ is given as

$$S_p(\omega) = S_a = \textit{constant}$$

$$= \frac{1}{2\pi}\int_{-\infty}^{\infty} R_p(\tau+\tau_1-\tau_2)\,\mathrm{e}^{-\mathrm{j}\omega(\tau+\tau_1-\tau_2)}\,\mathrm{d}\tau, \tag{34}$$

where

$$R_p(\tau+\tau_1-\tau_2) = E[p(t)\,p(t+\tau+\tau_1-\tau_2)]. \tag{35}$$

In equation (26), $G_i(t)$ with the white-noise excitation at m points known as the element nodal points becomes

$$G_i(t) = \left(\frac{420N^2}{\rho AL^2 D_i}\right) U_{mi}p(t). \tag{36}$$

Using equation (36), the autocorrelation function of $G_i(t)$ is expressed as

$$R_G(\tau+\tau_1-\tau_2) = E[G_i(t-\tau_1)G_k(t+\tau-\tau_2)]$$

$$= \left(\frac{420N}{l\rho AL}\right)^2 \frac{U_{mi}U_{mk}}{D_iD_k}\,R_p(\tau+\tau_1-\tau_2). \tag{37}$$

Substituting equations (34) and (37) into equation (32), we have

$$S_y(r,\omega) = H(r,\omega)H(r,-\omega)\,S_a, \tag{38}$$

where

$$H(r,-\omega) = \left(\frac{420N}{\rho AL}\right)\sum_{i=1}^{4N}\frac{U_{mi}U_{ri}}{D_i}\,H_i(-\omega), \tag{39}$$

$$H(r,\omega) = \left(\frac{420N}{\rho AL}\right)\sum_{k=1}^{4N}\frac{U_{mk}U_{rk}}{D_k}\,H_k(\omega). \tag{40}$$

Finally, the mean-square response $E[y^2]$ can be obtained as

$$E[y^2] = \int_{-\infty}^{\infty} H(r, \omega) H(r, -\omega) S_a \, \mathrm{d}\omega. \tag{41}$$

For the earthquake excitation, the Kanai–Tajimi earthquake model [12, 17] for the seismic analysis is used to model the base excitation of the rotating blade, the spectral function of the base acceleration $\ddot{y}_0$ is given as

$$S_0(\omega) = \left[\frac{\omega_0^4 + 4\zeta_0^2 \omega_0^2 \omega^2}{(\omega^2 - \omega_0^2)^2 + 4\zeta_0^2 \omega_0^2 \omega^2} \right] S_c$$

$$= \frac{1}{2\pi} \int_{-\infty}^{\infty} R_0(\tau + \tau_1 - \tau_2) \, \mathrm{e}^{-\mathrm{j}\omega(\tau + \tau_1 - \tau_2)} \, \mathrm{d}\tau, \tag{42}$$

where S_c is the spectrum level of the broadband excitation at the base, ω_0 is the natural frequency of the base, ζ_0 is the damping ratio of the base, and the autocorrelation function of the acceleration of the base is expressed as

$$R_0(\tau + \tau_1 - \tau_2) = E[\ddot{y}_0(t) \ddot{y}_0(t + \tau + \tau_1 - \tau_2)]. \tag{43}$$

For the earthquake excitation at the root, the $G_i(t)$ in equation (26) becomes

$$G_i(t) = \left(\frac{420N}{lD_i} \right) U_{mi} \ddot{y}_0(t). \tag{44}$$

Using equation (44), the autocorrelation function of $G_i(t)$ is expressed as

$$R_G(\tau + \tau_1 - \tau_2) = E[G_i(t - \tau_1) G_k(t + \tau - \tau_2)]$$

$$= \left(\frac{420N}{l} \right)^2 \frac{U_{mi} U_{mk}}{D_i D_k} R_0(\tau + \tau_1 - \tau_2). \tag{45}$$

Substituting equations (42) and (45) into equation (32), we have

$$S_y(r, \omega) = H(r, \omega) H(r, -\omega) S_0(\omega), \tag{46}$$

where

$$H(r, -\omega) = 420N \sum_{i=1}^{4N} \frac{U_{ri} U_{mi}}{D_i} H_i(-\omega), \tag{47}$$

$$H(r, \omega) = 420N \sum_{k=1}^{4N} \frac{U_{rk} U_{mk}}{D_k} H_k(\omega). \tag{48}$$

From equation (33), the mean-square response is expressed as

$$E[y^2] = \int_{-\infty}^{\infty} H(x, \omega) H(x, -\omega) S_0(\omega) \, \mathrm{d}\omega. \tag{49}$$

2.2. NON-STATIONARY RANDOM EXCITATION

The response y of equation (30) can be shown as

$$y = l \sum_{i=1}^{4N} U_{ri} \int_0^t G_i(\tau) h_i(t-\tau)\, \mathrm{d}\tau. \tag{50}$$

The non-stationary random excitation is presented by using the multiplicative description as [13, 23]

$$G(t) = V(t)\, g(t), \tag{51}$$

where $V(t)$ is a deterministic slowly varying function, and $g(t)$ is a stationary random process with zero mean and an autocorrelation function $R_G(\tau_2 - \tau_1)$.

The autocorrelation function of the response y is expressed as

$$R_y(r, t) = E[y^2(r, t)]$$

$$= l^2 \sum_{i=1}^{4N} \sum_{k=1}^{4N} U_{ri} U_{rk} \int_0^t \int_0^t h_i(t-\tau_1)\, h_k(t-\tau_2)\, V(\tau_1) V(\tau_2) R_G(\tau_2 - \tau_1)\, \mathrm{d}\tau_1\, \mathrm{d}\tau_2, \tag{52}$$

where $h_i(t-\tau_1)$ or $h_k(t-\tau_2)$ is given by equation (28), $R_G(\tau_2 - \tau_1)$ is given by equation (37) for the white-noise excitation and is given by equation (45) for the earthquake excitation, and $V(t)$ is taken as a unit step function or an exponentially decaying function $\mathrm{e}^{-\beta t}$, where β is not allowed to be too large so that $V(t)$ remains slowly varying.

3. RELIABILITY ANALYSIS

Reliability in a dynamic case is defined as the probability that the blade is not failing within a specified time interval. We assume that the blade fails if the deflection y exceeds some specific value y_a. In the literature, this problem is referred to as the first passage problem.

3.1. STATIONARY PROCESS

The reliability of the blade in a stationary process is given by [21–23]

$$Rel = \exp[-vt], \tag{53}$$

where v is the expected rate of up-crossing the threshold y_a, given by

$$v = \frac{\sigma_{\dot{y}}}{2\pi\sigma_y} \exp\left[-\frac{y_a^2}{2\sigma_y^2}\right], \tag{54}$$

where the variance σ_y^2 is equal to the mean square response $E[y^2]$, and $\sigma_{\dot{y}}$ is the root-mean-square transverse velocity.

3.2. NON-STATIONARY PROCESS

The reliability of the blade subjected to non-stationary excitation is represented as

$$Rel = \exp\left[-\int_0^t v \, dt \right], \tag{55}$$

where

$$v = \frac{\sigma_{\dot{y}}(t)}{2\pi\sigma_y(t)} \exp\left[-\frac{y_a^2}{2\sigma_y^2(t)} \right]. \tag{56}$$

4. NUMERICAL RESULTS AND DISCUSSION

A rotating cantilever blade subjected to the stationary random excitation is studied by using the finite element method. The end mean square responses of a rotating cantilever blade with $S_a = 0{\cdot}000575(\rho AL)^2$ N^2/Hz, $S_c = 0{\cdot}000575$ m^2/s^4 Hz^{-1}, $\omega_0^2 = 242 \times 10^6$ 1/s^2, $\zeta_0 = 0{\cdot}6398$, $C_0 = 0{\cdot}02 \times 10^{-6}$ s/m^4 and $e = 4$ are presented in Table 1. The results show that the present finite element method solutions have good convergence. The good agreement of the present finite element method solutions with those of modal analysis and Galerkin's method demonstrates that the present calculations have excellent accuracy.

The effects of the simplified external damping coefficient on the mean-square response are shown in Figure 2. As expected, the increment of external damping reduces the mean-square response. It is seen that the influence of white-noise excitation at the free end and earthquake excitation at the root are quite different. The simplified external damping coefficient in the range $0{\cdot}02 \times 10^{-6} < C_0 < 0{\cdot}1 \times 10^{-6}$ has a significant effect on the mean-square response under white noise and earthquake excitations.

TABLE 1

Convergence of the mean-square response (mm$^2 \times 10^{-3}$) *of the free end of a blade by the finite element method with* $S_a = 0{\cdot}000575(\rho AL)^2$ N^2/Hz, $S_c = 0{\cdot}000575$ m^2/s^4 Hz^{-1}, $\omega_0^2 = 242 \times 10^6$ 1/s^2, $\zeta_0 = 0{\cdot}6398$, $C_0 = 0{\cdot}02 \times 10^{-6}$ s/m^4, $e = 4$[†]

No. of elements N	White noise-excitation at the free end		Earthquake excitation at the root	
	Non-rotating $\mu = 0$	Rotating $\mu = 0{\cdot}6$	Non-rotating $\mu = 0$	Rotating $\mu = 0{\cdot}6$
2	12·1076 (0·0055)[‡]	8·90382 (0·0181)	1·98994 (0·0014)	1·50311 (0·0090)
3	12·0636 (0·0019)	8·86678 (0·0139)	1·98571 (− 0·0007)	1·49990 (0·0068)
4	12·0525 (0·0010)	8·85707 (0·0128)	1·98459 (− 0·0013)	1·49899 (0·0062)
5	12·0483 (0·0006)	8·85333 (0·0123)	1·98424 (− 0·0014)	1·49871 (0·0060)
a	12·0409	—	1·98712	—
b	12·0409	8·74556	1·98712	1·48977

[†] a, modal analysis solution [13]. b, Galerkin's method solution [24].
[‡] Percentage error with respect to Galerkin's solution.

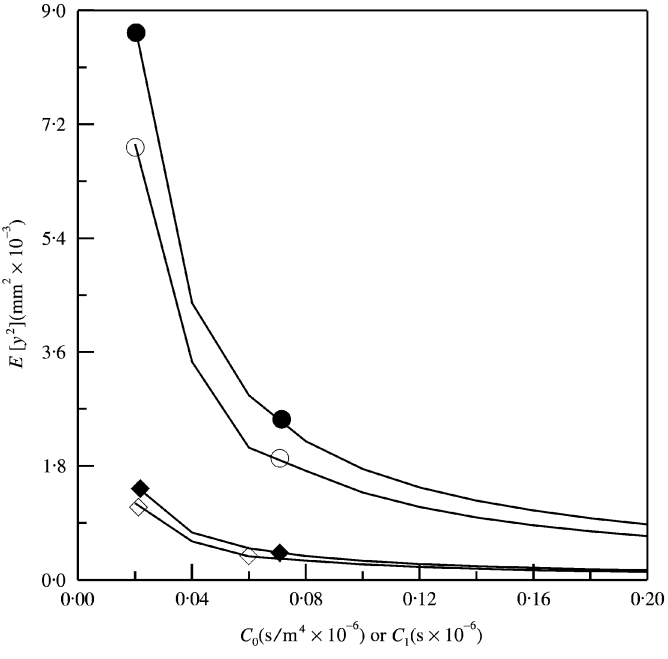

Figure 2. The mean-square response at the free end of a rotating blade versus the simplified external or internal damping coefficient ($e = 4$, $\mu = 0{\cdot}6$): (a) white-noise excitation at the free end with $S_a = 0{\cdot}000575(\rho AL)^2$ N^2/Hz, —●—, C_0; —○—, C_1; (b) earthquake excitation at the root with $S_c = 0{\cdot}000575$ m^2/s^4 Hz^{-1}, $\omega_0^2 = 242 \times 10^6$ 1/s^2, $\zeta_0 = 0{\cdot}6398$, —◆—, C_0; —◇—, C_1.

Figure 2 also presents the effect of simplified internal damping coefficient on the square response under white-noise and earthquake excitations. It is also shown that the mean-square response will monotonously decrease when the internal damping increases. For white-noise and earthquake excitations, the simplified internal damping coefficient in the range $0{\cdot}02 \times 10^{-6} < C_1 < 0{\cdot}1 \times 10^{-6}$ has also a significant effect on the mean-square response. The effects of simplified external and internal damping coefficient on the square response under white-noise and earthquake excitations are considered in Figure 3. As it is clearly seen, the mean-square response decreases when the internal and external damping increase at the same time.

For the white-noise and earthquake excitations, the effects of the simplified internal damping coefficient and rotational speed on the mean-square response at the free end of a rotating blade are shown in Figure 4(a) and 4(b) respectively. It is seen that the influence of simplified internal damping coefficient on the mean-square response decreases when rotational speed increases.

Figure 5 presents the effects of the simplified external damping coefficient and rotational speed on the mean-square response at the free end of a rotating blade for the earthquake excitation of the root. It is again shown that the effect of simplified external damping coefficient on the mean-square response decreases when the rotational speed increases. The results indicate that the increments of rotational speed and damping become the forces of resistance which act on the blade, and cause the reduction of the mean-square response.

Figure 6 shows the effects of the simplified internal damping coefficient and the low natural frequency ω_0 of base ($\omega_0 <$ the first natural frequency $\omega_1 = 4{\cdot}10384 \times 10^3$ 1/s of rotating cantilever beam) on the mean-square response at the free end of a rotating blade for the earthquake excitation of the root. It is found that the mean-square response decreased

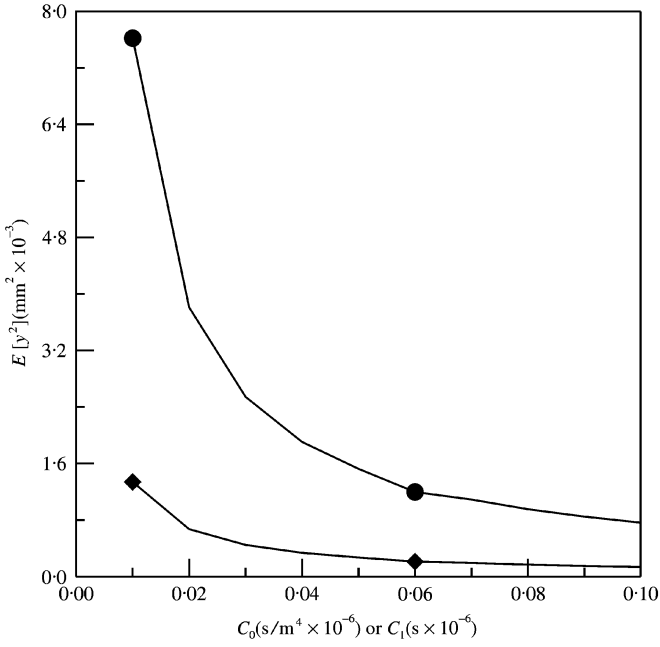

Figure 3. The mean-square response at the free end of a rotating blade versus the simplified external and internal damping coefficient ($e = 4$, $\mu = 0{\cdot}6$): (a) white-noise excitation at the free end with $S_a = 0{\cdot}000575(\rho AL)^2\ \text{N}^2/\text{Hz}$, (—●—); (b) earthquake excitation at the root with $S_c = 0{\cdot}000575\ \text{m}^2/\text{s}^4\ \text{Hz}^{-1}$, $\omega_0^2 = 242 \times 10^6\ 1/\text{s}^2$, $\zeta_0 = 0{\cdot}6398$, (—◆—).

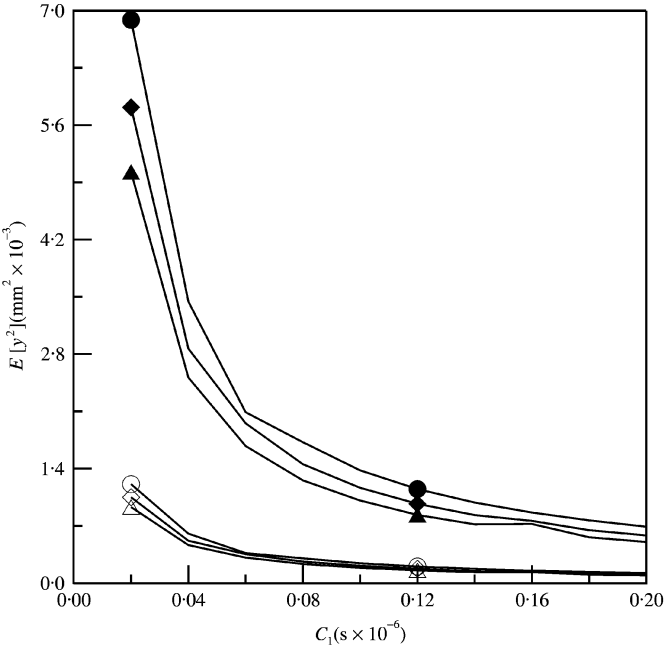

Figure 4. Effects of the simplified internal damping coefficient and rotational speed on the mean-square response at the free end of a rotating blade: (a) white-noise excitation of free end ($e = 4$, $S_a = 0{\cdot}000575(\rho AL)^2\ \text{N}^2/\text{Hz}$), ($\mu$ — —●—, 0·6; —◆—, 1·0; —▲—, 1·4); (b) earthquake excitation of the root ($e = 4$, $S_c = 0{\cdot}000575\ \text{m}^2/\text{s}^4\ \text{Hz}^{-1}$, $\omega_0^2 = 242 \times 10^6\ 1/\text{s}^2$, $\zeta_0 = 0{\cdot}6398$), (μ — —○—, 0·6; —◇—, 1·0; —△—, 1·4).

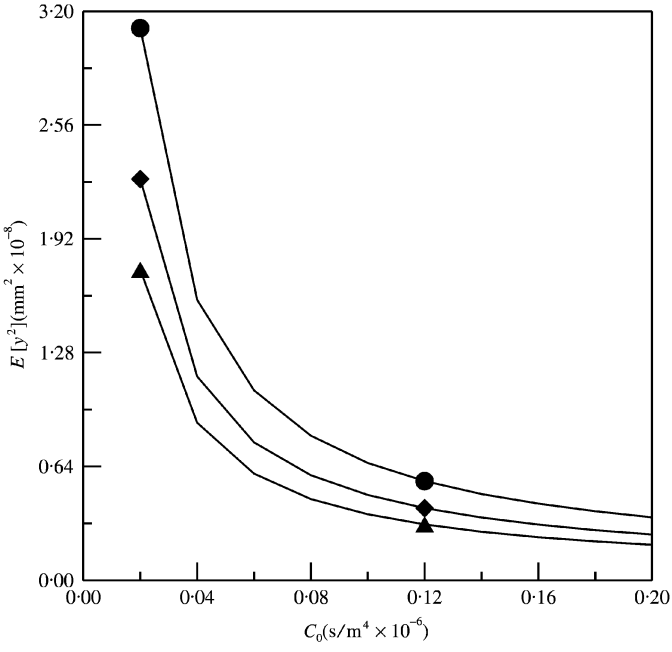

Figure 5. Effects of the simplified external damping coefficient and rotational speed on the mean-square response at the free end of a rotating blade for the earthquake excitation of the root ($e = 4$, $S_c = 0{\cdot}000575\ \text{m}^2/\text{s}^4\,\text{Hz}^{-1}$, $\omega_0^2 = 242\ 1/\text{s}^2$, $\zeta_0 = 0{\cdot}6398$): (μ — —●—, 0·6; —◆—, 1·0; —▲—, 1·4).

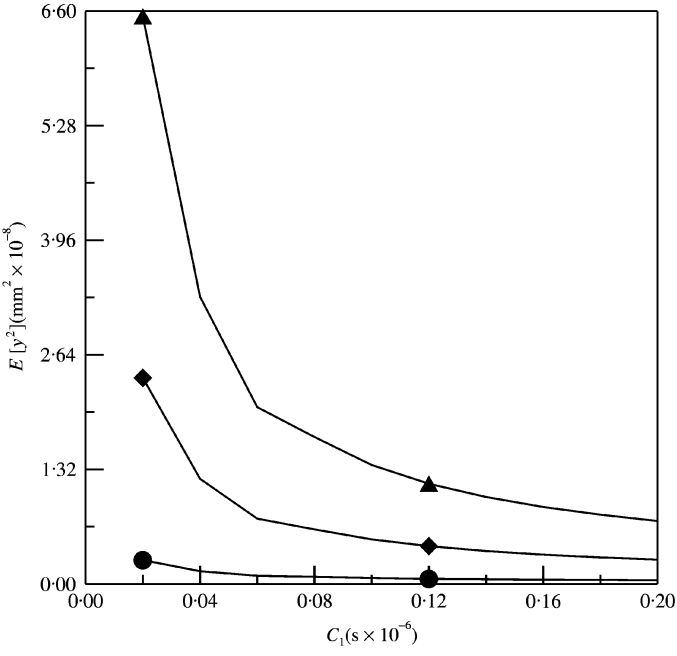

Figure 6. Effects of the simplified internal damping coefficient and the low natural frequency of base on the mean-square response at the free end of a rotating blade for the earthquake excitation of the root ($e = 4$, $\mu = 0{\cdot}6$, $S_c = 0{\cdot}000575\ \text{m}^2/\text{s}^4\,\text{Hz}^{-1}$, $\zeta_0 = 0{\cdot}6398$): (ω_0(1/s) — —●—, 5; —◆—, 15; —▲—, 25).

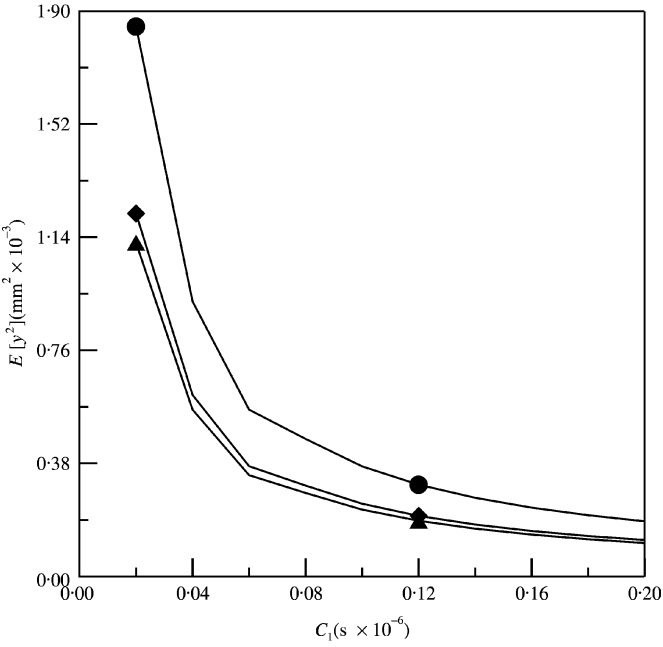

Figure 7. Effects of the simplified internal damping coefficient and the high natural frequency of base on the mean-square response at the free end of a rotating blade for the earthquake excitation of the root ($e = 4$, $\mu = 0{\cdot}6$, $S_c = 0{\cdot}000575\ \text{m}^2/\text{s}^4\,\text{Hz}^{-1}$, $\zeta_0 = 0{\cdot}6398$): ω_0(1/s) — —●—, 5000; —◆—, 15 000; —▲—, 25 000.

when the low natural frequency of base decreases. Inversely, for the high natural frequency of base $\omega_0 > \omega_1$, it can be seen in Figure 7 that the mean-square response increases when the high natural frequency of base decreases.

Figure 8 shows that the mean square response is constant at $0{\cdot}7181 \times 10^{-3}\ \text{mm}^2$ for stationary white-noise excitation and gradually approaches the constant value after $t = 3{\cdot}2$ s from zero for non-stationary case.

Figure 9 presents the results for $y_a = 0{\cdot}05$ and $0{\cdot}06$ mm, with time (s) shown in a logarithmic scale under the earthquake excitation. It can be seen that the reliability level of 0·95, for example, is obtained at $t = 15{\cdot}63$ s for $y_a = 0{\cdot}05$ mm and at $t = 161{\cdot}2$ s for $y_a = 0{\cdot}06$ mm. It should be noted that this difference is due to an increase of only 20% in y_a. The reliability at $t = 10$ s of the blade with different S_c is shown in Figure 10 for $y_a = 0{\cdot}05$ and 0·06 mm. It is seen that for a specific y_a, the reliability decreases with the increase of S_c.

Figure 11 shows the results for the stationary white-noise excitation. It is found that the reliability level of 0·95 is obtained at $t = 2{\cdot}512$ s for $y_a = 0{\cdot}05$ mm and at $t = 11{\cdot}63$ s for $y_a = 0{\cdot}06$ mm. For the non-stationary white-noise excitation modulated by a unit step function, Figure 12 shows that the reliability level of 0·95 is obtained at $t = 4{\cdot}584$ s for $y_a = 0{\cdot}05$ mm and at $t = 21{\cdot}05$ s for $y_a = 0{\cdot}06$ mm. For the case of stationary and non-stationary white-noise excitation, the reliability at $t = 10$ s of the blade with different μ is shown in Figure 13(a) and 13(b) respectively. It is seen that for a specific y_a, the reliability increases with the increase of μ.

5. CONCLUSIONS

The present finite element model is shown to be an effective method and to have good accuracy for the analysis of random vibration of a rotating blade. It is found that the

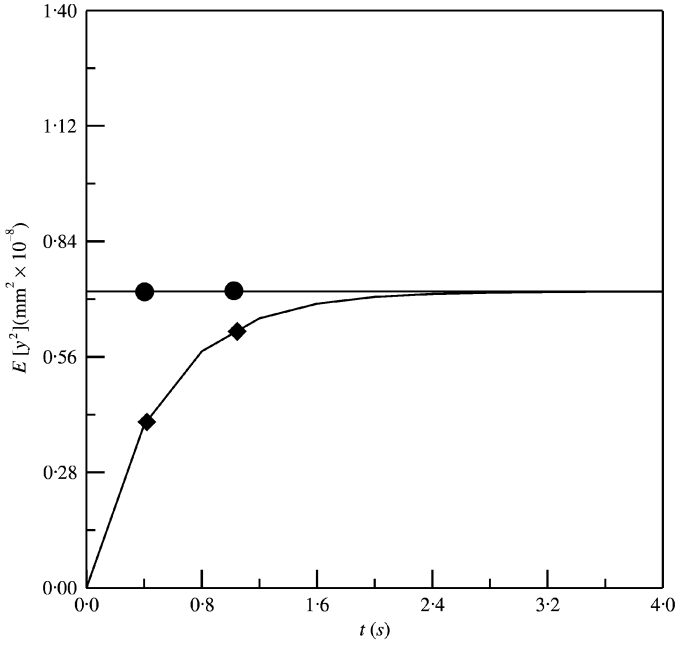

Figure 8. The mean-square response at the free end of a rotating blade versus time ($e = 4$, $\mu = 0{\cdot}6$, $C_1 = 0{\cdot}1 \times 10^{-6}$ s, $S_a = 0{\cdot}0003(\rho AL)^2$ N^2/Hz): (a) stationary white-noise excitation, (—●—); (b) non-stationary white-noise excitation modulated by a unit step function, (—◆—).

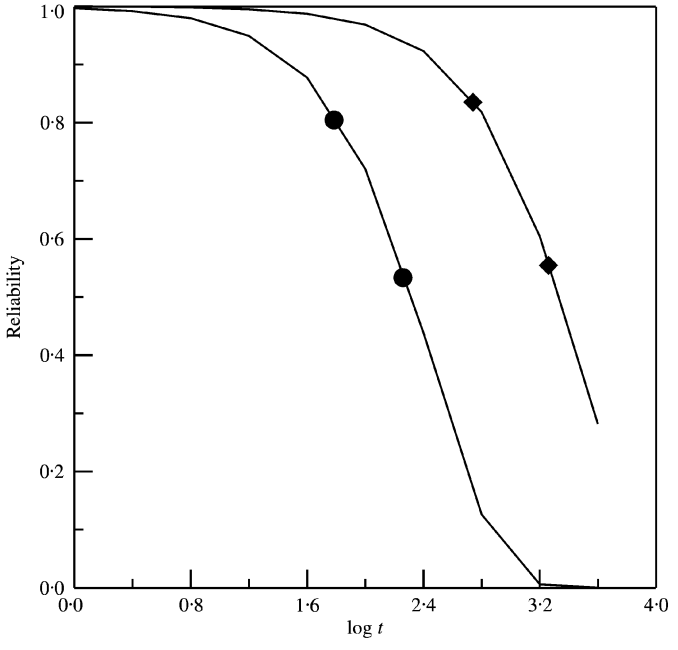

Figure 9. Reliability versus time for the stationary earthquake excitation of root with $e = 4$, $\mu = 0{\cdot}6$, $C_1 = 0{\cdot}1 \times 10^{-6}$ s, $S_c = 0{\cdot}000575$ m^2/s^4 Hz^{-1}, $\omega_0^2 = 242$ 1/s^2, $\zeta_0 = 0{\cdot}6398$: y_a(mm) — —●—, 0·05; —◆—, 0·06.

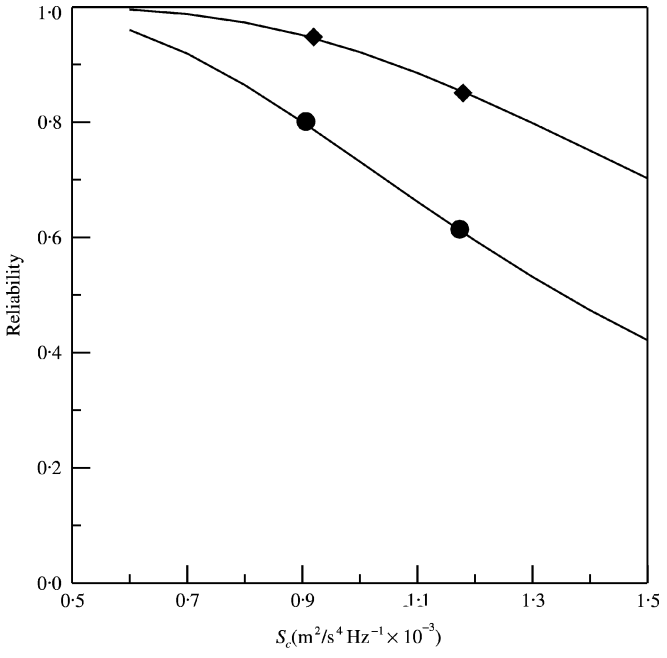

Figure 10. Reliability versus the earthquake excitation spectrum level with $t = 10$ s, $e = 4$, $\mu = 0{\cdot}6$, $C_1 = 0{\cdot}1 \times 10^{-6}$ s, $S_c = 0{\cdot}000575\ m^2/s^4\,Hz^{-1}$, $\omega_0^2 = 242\ 1/s^2$, $\zeta_0 = 0{\cdot}6398$: y_a(mm) — —●—, 0·05; —◆—, 0·06.

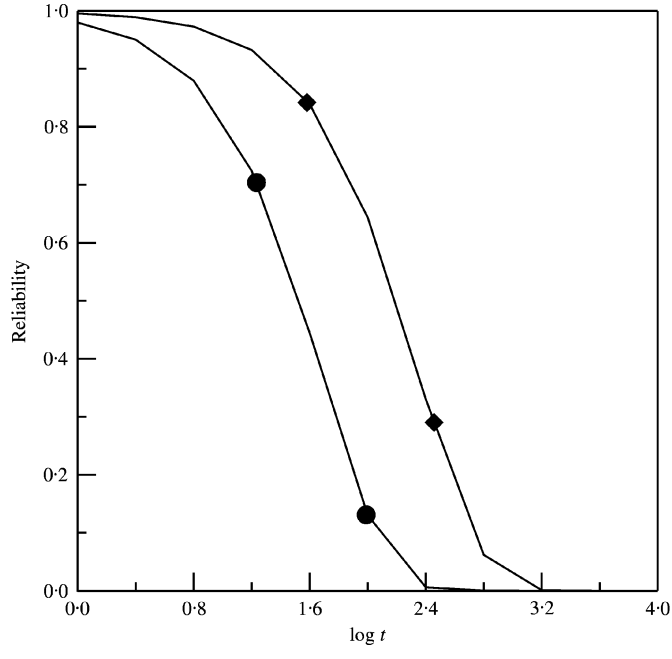

Figure 11. Reliability versus time for the stationary white noise excitation of free end with $e = 4$, $\mu = 0{\cdot}6$, $C_1 = 0{\cdot}1 \times 10^{-6}$ s, $S_a = 0{\cdot}00015(\rho AL)^2\ N^2/Hz$: y_a(mm) — —●—, 0·05; —◆—, 0·06.

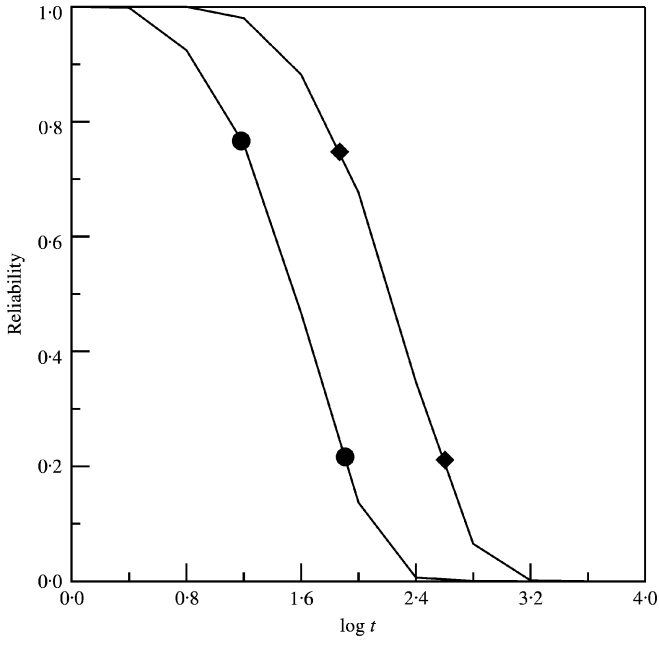

Figure 12. Reliability versus time for the non-stationary white-noise excitation modulated by a unit step function with $e = 4$, $\mu = 0{\cdot}6$, $C_1 = 0{\cdot}1 \times 10^{-6}$ s, $S_a = 0{\cdot}00015(\rho AL)^2$ N^2/Hz: y_a(mm) — —●—, 0·05; —◆—, 0·06.

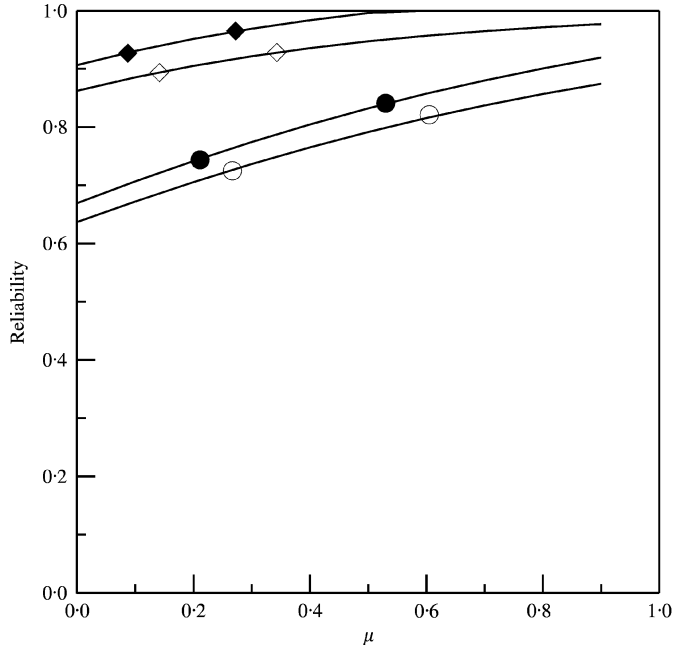

Figure 13. Reliability versus the rotational speed: (a) stationary, (y_a(mm) — —○—, 0·05; —◇—, 0·06); (b) non-stationary, (y_a(mm) — —●—, 0·05; —◆—, 0·06) white-noise excitation modulated by a unit step function with $e = 4$, $\mu = 0{\cdot}6$, $C_1 = 0{\cdot}1 \times 10^{-6}$ s, $S_a = 0{\cdot}00015(\rho AL)^2$ N^2/Hz.

external and internal damping have a significant effect on the mean-square response. As expected, the increment of damping and rotational speed will reduce the random response of a rotating blade, and cause the increase of reliability. Moreover, the mean-square response decreases when the low natural frequency of base decreases. Inversely, for the case that the high natural frequencies of base are over the first natural frequency of blade, the mean-square response increases when the high natural frequency of base decreases. In engineering design, the present calculations of the rotating blade reliability under the random excitation are important to presume the instability or fatigue of the system due to the over-random response.

REFERENCES

1. W. CARNEGIE 1959 *Journal of Mechanical Engineering Sciences* **1**, 235–240. Vibrations of rotating cantilever blading: theoretical approaches to the frequency problem based on energy methods.
2. W. CARNEGIE, C. STIRLING and J. FLEMING 1966 *Proceedings of the Institution of Mechanical Engineers* **180**, 1–9. Vibration characteristics of turbine blading under rotation results of an initial investigation and details of high speed test installation.
3. W. CARNEGIE and J. S. RAO 1971 *Bulletin of Mechanical Engineering Education* **10**, 239. Effect of pretwist and rotation on flexural vibrations of cantilever beams treated by the extended holzer method.
4. R. M. KRUPKA and A. M. BAUMANIS 1969 *Journal of Engineering for Industry American Society of Mechanical Engineers* **91**, 1017–1028. Bending–bending mode of a rotating tapered twisted turbomachine blade including rotary inertia and shear deflection.
5. R. O. STAFFORD and V. GIURGIUTIU 1975 *International Journal of Mechanical Sciences* **17**, 719–727. Semi-analytic methods for rotating Timoshenko beams.
6. B. A. H. ABBAS 1979 *Aeronautical Journal* **83**, 450–453. Simple finite elements for dynamic analysis of thick pre-twisted blades.
7. J. THOMAS and B. A. H. ABBAS 1975 *Journal of Sound and Vibration* **41**, 291–299. Finite element model for dynamic analysis of Timoshenko beam.
8. L. W. CHEN and C. L. CHEN 1988 *Computers and Structures* **28**, 67–74. Vibration and stability of cracked thick rotating blades.
9. L. W. CHEN and C. L. CHEN 1990 *Computers and Structures* **35**, 653–660. Non-conservative stability of a cracked thick rotating blade.
10. E. S. ZORZI and H. D. NELSON 1977 *Journal of Engineering for Power* **99**, 71–76. Finite element simulation of rotor-bearing systems with internal damping.
11. T. FANG and Z. N. WANG 1986 *American Institute of Aeronautics and Astronautics Journal* **24**, 860–862. Mean square response to band-limited white noise excitation.
12. T. FANG and Z. N. WANG 1986 *American Institute of Aeronautics and Astronautics Journal* **24**, 1048–1051. Stationary response to second-order filtered white-noise excitation.
13. G. AHMADI and M. A. SCATTER 1975 *American Institute of Aeronautics and Astronautics Journal* **13**, 1097–1100. Mean-square response of beams to nonstationary random excitation.
14. C. LEE and R. SINGH 1994 *Journal of Sound and Vibration* **174**, 379–394. Analysis of discrete vibratory systems with parameter uncertainties. Part I: eigensolution.
15. I. ELISHAKOFF, Y. K. LIN and C. P. ZHU 1995 *Computer Methods in Applied Mechanics and Engineering* **121**, 59–75. Random vibration of uniform beams with varying boundary conditions by the dynamic-edge-effect method.
16. Z. FANG 1995 *Computers and Structures* **55**, 1037–1044. Dynamic analysis of structures with uncertain parameters using the transfer matrix method.
17. Y. K. LIN, F. ASCE and Y. YONG 1987 *Journal of Engineering Mechanics* **113**, 1119–1136. Evolutionary Kanai–Tajimi earthquake models.
18. R. S. JANGID and T. K. DATTA 1995 *Journal of Sound and Vibration* **179**, 463–473. The stochastic response of asymmetric base isolated buildings.
19. I. ELISHAKOFF and L. ZHU 1993 *Computer Methods in Applied Mechanics and Engineering* **105**, 359–373. Random vibration of structures by the finite element method.
20. R. RACKWITZ and B. FIESSLER 1978 *Computers and Structures* **9**, 489–494. Structural reliability under combined random load sequences.

21. A. B. MASON and W. D. IWAN 1983 *Journal of Applied Mechanics* **50**, 641–646. An approach to the first passage problem in random vibration.
22. R. S. LANGLEY 1988 *Journal of Sound and Vibration* **122**, 261–275. A first passage approximation for normal stationary random processes.
23. G. CEDERBAUM, I. ELISHAKOFF, J. ABOUD and L. LIBRESCU 1992 *Random Vibration and Reliability of Composite Structures*. New Holland Avenue: Technomic Publishing Company.
24. I. ELISHAKOFF 1983 *Probabilistic Methods in the Theory of Structures*. New York: John Wiley & Sons.

APPENDIX A

$$M_e = \frac{\rho A l^3}{420}\begin{bmatrix} 156 & 22 & 54 & -13 \\ & 4 & 13 & -3 \\ \textit{symmetric} & & 156 & -22 \\ & & & 4 \end{bmatrix},$$

$$C_e = \frac{EI}{420l}[C_{ij}], \quad C_{ij} = C_{ji},\ i \text{ and } j = 1,2,3,4,$$

$$K_e = \frac{EI}{420l}[K_{ij}], \quad K_{ij} = K_{ji},\ i \text{ and } j = 1,2,3,4,$$

where

$$C_{11} = 156C_0l^4 + 5040C_1, \qquad C_{12} = 22C_0l^4 + 2520C_1,$$

$$C_{13} = 54C_0l^4 - 5040C_1, \qquad C_{14} = -13C_0l^4 + 2520C_1,$$

$$C_{22} = 4C_0l^4 + 1680C_1, \qquad C_{23} = 13C_0l^4 - 2520C_1,$$

$$C_{24} = -3C_0l^4 + 840C_1, \qquad C_{33} = 156C_0l^4 + 5040C_1,$$

$$C_{34} = -22C_0l^4 - 2520C_1, \qquad C_{44} = 4C_0l^4 + 1680C_1,$$

$$K_{11} = 5040 + 180S_1 + 252S_3 + 504S_4,$$

$$K_{12} = 2520 + 6S_1 + 42S_4,$$

$$K_{13} = -5040 - 180S_1 - 252S_3 - 504S_4,$$

$$K_{14} = 2520 + 27S_1 + 42S_3 + 42S_4,$$

$$K_{22} = 1680 + 24S_1 + 42S_3 + 56S_4,$$

$$K_{23} = -2520 - 6S_1 - 42S_4, \qquad K_{24} = 840 - 4S_1 - 7S_3 - 14S_4,$$

$$K_{33} = 5040 + 180S_1 + 252S_3 + 504S_4,$$

$$K_{34} = -2520 - 27S_1 - 42S_3 - 42S_4,$$

$$K_{44} = 1680 + 10S_1 + 14S_3 + 56S_4.$$